Effective Stress Analysis of a Soil-Pile-Hammer System During Pile Driving

M. Ghazavi
B.A, M.Sc.
Research student, The University of Queensland, Australia
D.J. Williams
B.E., Ph.D., M.I.E.Aust.
Associate Professor, Department of Civil Engineering, The University of Queensland, Australia
K.Y. Wong
B.E., Ph.D., F.I.E.Aust.
Technical Director, L & M Geotechnic Sdn. Bnd., Malaysia

Summary A one-dimensional finite element analysis of a soil-pile-hammer system during pile driving is presented. The pile hammer is modelled using the approach of Smith (1960). The pile is assumed to behave elastically, and is discretised into a number of simple linear elements connected by nodes. The soil resistance acting at each pile node is modelled by a spring and a dashpot, and the shear resistance of the soil is calculated using the Mohr-Coulomb failure criterion. The resistance of the soil incorporates a non-linear exponential function to account for rate effects associated with pile driving. The excess pore pressures generated along the shaft, resulting from shear stresses and changes in total stress are computed. The results are compared with field measurements obtained from a fully instrumented pile driven in a saturated overconsolidated clay. These comparisons show that the model predicts the sets and stresses generated by driving well.

1. INTRODUCTION

Early pile driving analyses were empirically-based and unreliable. The subsequent more soundly-based wave equation method focussed on the transmission of energy from the hammer to the pile.

Limited attempts have so far been made to analyse pile driving by three-dimensional or axisymmetric finite element calculations. However, these are very time consuming and rather expensive, and are impractical in many situations. This paper applies a simple one-dimensional wave equation to pile driving, using a standard finite element algorithm. The soil is assumed to be elasto-plastic, with a limiting shear resistance determined from the effective stress parameters at the soil-pile interface, rather than the more usual empirically-based criteria.

2. METHOD OF ANALYSIS

The pile is idealised as a number of linear elastic elements connected by nodes. The soil resistances along the embedded pile shaft and at the pile tip are incorporated using the elasto-dynamic theory of Novak et al. (1978). The hammer, cushion, and other elements such as the capblock, are represented by a series of weights and springs (Smith, 1960). The soil-pile-hammer idealisation is shown on Figure 1. The governing dynamic differential equation for a soil-pile-hammer system is discretised over the entire length of the pile and then assembled, using the standard finite element method (Smith, 1988). The global equation of the soil-pile-hammer system in matrix form can be solved numerically, using the time-stepping Newmark-β method (Bathe and Wilson, 1976).

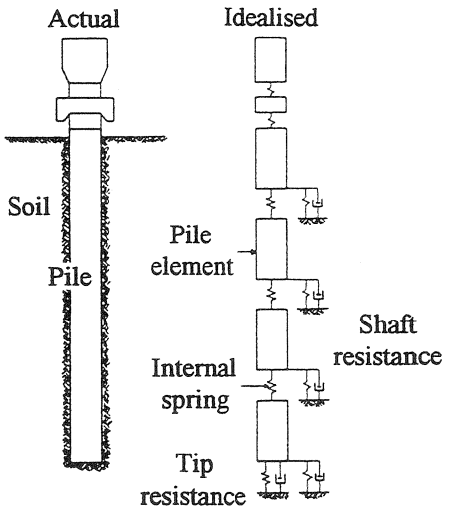

Figure 1. Idealisation of soil-pile-hammer system.

3. RATE EFFECTS

The well-known dependence of the resistance of soil on the rate of loading is a non-linear phenomenon which is frequently represented by a power law. Soil-soil and soil-pile interface resistances generally increase when the rate of shearing increases, particularly for clayey soil. For sandy soil, this effect is negligible.

In soil-pile systems, the soil at the interface, both along the shaft and at the tip, is also subjected to time-varying stresses. This effect should also be incorporated in a soil resistance model. For example, Smith (1960) incorporated a representing viscous resistance in his conventional wave equation analysis of pile driving. A laboratory investigation by Litkouhi and Poskitt (1980) of rate effects on the strength of silty clays ranging from normally consolidated or lightly overconsolidated to very stiff, revealed that during the penetration of a model pile, the resistance of the soil behaved according to the power law

$$R_d = R_s.(1 + J.V^N) \qquad (1)$$

where R_d is the dynamic resistance, R_s is the ultimate static resistance, V is the penetration rate of the model pile, J represents the rate effects and N accounts for the non-linear behaviour.

Litkouhi and Poskitt (1980) proposed that the non-linear damping of the clayey soil be considered in the wave equation analysis. They also found that the pile shaft damping values were greater than those of the pile tip, contradicting Smith (1960). Coyle and Gibson (1970) conducted triaxial impact tests to determine the soil damping parameter for a sand and a clay. They obtained values of 0.2 and 0.18 for the sand and clay, respectively.

Guidance on values for J and N for the pile shaft and tip, particularly in the absence of other data, was presented by Lee et al. (1988) who compiled data from a number of sources.

4. SOIL RESISTANCE

4.1 Elastic Resistance

It has been well established by the elasto-dynamic analysis of driven piles that elastic waves generated at the soil-pile interface propagate in the horizontal direction (Novak, 1974). Under plane strain conditions, and so long as the soil remains in the elastic range, the shaft resistance to pile motion at depth z, $P_s(z)$, is commonly expressed in terms of the impedance functions

$$P_s(z) = G_s.(S_{w1} + i.S_{w2}).w(z) \qquad (2a)$$

$$P_s(z) = (k_1 + k_2).w(z) \qquad (2b)$$

where G_s is the soil shear modulus; S_{w1} and S_{w2} are functions of the dimensionless frequency $a_o = r_o.\omega/V_s$, in which r_o is the pile radius, ω is the circular frequency of excitation, V_s is the shear wave velocity in the soil given by $\sqrt{(G_s/\rho_s)}$, ρ_s is the soil density; $i = \sqrt{-1}$; w(z) is the nodal displacement; k_1 represents the soil stiffness; and k_2 represents an imaginary component which accounts for energy dissipation in the soil. Because damping generally increases with increasing frequency, and hence resembles viscous damping, it can also be defined in terms of a constant equivalent viscous damping. The force-displacement equation then becomes

$$P_s(z) = k.w(z).+ c.\frac{w(z)}{dt} \qquad (3)$$

where both k and c are real constants.

The variation of S_{w1} and S_{w2} with the dimensionless frequency are illustrated on Figure 2 (Novak, 1974), which shows that at higher dimensionless frequencies the values of S_{w1} and S_{w2}/a_o do not vary significantly and approach 2.75 and 2π, respectively (Lee et al., 1988). Substituting for ω gives the soil resistance along the pile shaft in the elastic range in terms of frequency-independent parameters as

$$P(z) = 2.75\ G_s.w(z) + 2\pi.r_o.\sqrt{(G_s.\rho_s)}.\frac{w(z)}{dt} \qquad (4)$$

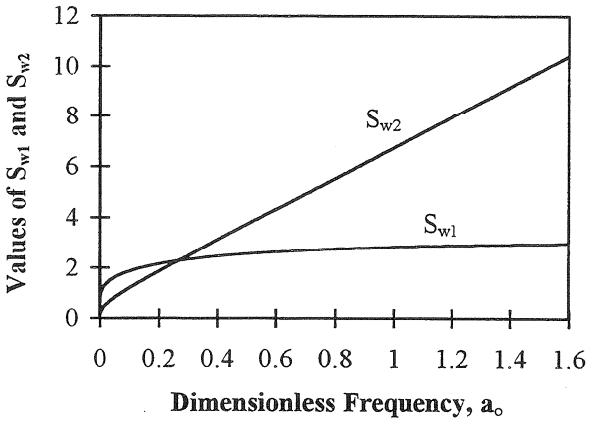

Figure 2. Variation of S_{w1} and S_{w2} with dimensionless frequency a_o (after Novak, 1974).

The tip resistance of a close-ended pile is approximated by that of a vertically vibrating rigid disc on top of an elastic half-space, using Lysmer's analog (Lysmer and Richart, 1966)

$$P_b = (4\ G_s.r_o.w_b)/(1 - \nu_s) + [3.4\ r_o^2.\sqrt{(G_s.\rho_s)}.v_b]/(1 - \nu_s) \qquad (5)$$

where w_b and v_b represent the tip displacement and velocity, respectively. For open-ended piles, using the soil stiffness at the pile tip based on the approximation of Egorov (1965), and the radiation (geometric) damping coefficient for a ring (Gazetas and Dobry, 1984), the soil tip resistance to pile motion in the elastic range is

$$P_b = (2\ G_s.r_o.w_b)/[(1 - \nu_s).\Omega(\eta)] + [3.4\ (r_o^2 - r_i^2).\sqrt{(\ G_s.\rho_s)}]/(1 - \nu_s) \qquad (6)$$

where ν_s is the Poisson's ratio for the soil, $\eta = r_i/r_o$, r_i and r_o are the inner and outer radii of the pile, respectively, and Ω is a constant dependent on η.

4.2 Ultimate Resistance

Recent field tests carried out on fully instrumented piles jacked into normally to highly overconsolidated clays have shown that the ultimate shaft resistance is controlled by the effective stresses in the soil. Lee et al. (1988) considered that soil failure occurs only when the soil spring force reaches its dynamic limit, which has been determined from the static limit by incorporating rate effects. Herein, the same criterion is adopted. However, it is assumed that the ultimate static resistance of the soil spring is reached when the stress state satisfies the Mohr-Coulomb failure criterion

$$\tau_f = c_a' + \sigma_n'.\tan\delta \qquad (7)$$

where τ_f is the ultimate static skin friction developed along the interface, c_a' is the effective adhesion between the pile and the soil, $\sigma_n'.\tan\delta$ is the effective friction developed at the interface, σ_n' is the effective stress normal to the pile face, and δ is the angle of friction between the pile and the soil.

The adhesion is normally reduced to a low value by the remoulding effects which accompany pile installation and may be ignored. The values of c_a' and δ are strongly dependent on the soil type, the surface roughness of the pile, and the stress state in the soil.

The ultimate static resistance of the soil at the pile tip is herein assumed to be given by the conventional value of 9 c_u, where c_u is the undrained shear strength of the soil.

Since a direct measurement of σ_n' is impossible, it is determined using the principle of effective stress. Consequently, a knowledge of the total radial stress and the pore pressure is essential.

4.3 Radial Stresses

The initial radial total stress (prior to a hammer blow) may be expressed by

$$\sigma_r = m_1.\sigma_v \qquad (8)$$

where σ_r is the radial total stress and σ_v is the vertical total stress, the two related by m_1. It can be shown that the increment in the radial total stress due to the plane strain expansion and contraction of the pile cross-section (induced by the Poisson's ratio effect) during one hammer blow may be expressed by

$$\Delta\sigma_r = 2\, G_s.\nu_p.\Delta\varepsilon_p \qquad (9)$$

where ν_p is the Poisson's ratio of the pile material, and $\Delta\varepsilon_p$ is the increment of axial strain developed in the pile. Equation (9) is applied at each node. Due to the very short duration of a hammer blow, it is reasonable to assume that the degree of relaxation of the radial total stress along the shaft is negligible. Therefore; the Poisson's ratio of the pile material is the only significant generator of radial total stresses, which in turn generate excess pore pressures.

4.4 Pore Pressures

In the pile driving model, the pore pressure u immediately prior to the next hammer blow is required. This may be calculated from

$$u = m_2.u_o \qquad (10)$$

where u_o is the hydrostatic pore pressure, and m_2 varies with the time elapsed since the previous hammer blow and with the soil type. During the analysis of a single hammer blow, undrained conditions are assumed to prevail, due to the rapid rate of loading. The total pore pressure at any depth and time can be calculated by summing the initial value and the increments of pore pressure generated within the time interval.

Henkel (1960) proposed the expression for the excess pore pressure in a soil element under undrained conditions

$$\Delta u = B^*.\Delta\sigma_{oct} + A^*.\Delta\tau_{oct} \qquad (11)$$

where for fully saturated soils $B^* \cong 1$ (Bjerrum, 1969), $\Delta\sigma_{oct}$ is the change in octahedral stress, $\Delta\tau_{oct}$ is the change in octahedral shear stress, and

$$A^* = (3\,A - 1)/\sqrt{2} \qquad (12)$$

where A is Skempton's pore pressure parameter determined using triaxial test data. Negative values for A^* are expected for overconsolidated soil, which dilates on shearing.

Using Equation (11), strain compatibility, and equilibrium equations, it can be shown that the pore pressure generated at a given depth and within a given time interval following a hammer blow, Δu_g, is given by

$$\Delta u_g = A^*.\sqrt{6}/3\ \sqrt{(\Delta\sigma_r^2 + \Delta\tau_{rz}^2)} \qquad (13)$$

where $\Delta\tau_{rz}$ is the shear stress in the r, z-plane.

5. SUMMARY OF THE MODEL

In the pile driving model, the increments of radial total stress and pore pressure at nodes along the pile shaft are computed within each time interval and added to the pre-existing radial total stresses and pore pressures. The effective stress normal to the pile face is then calculated, using the principle of effective stress. The ultimate static shaft resistance is determined, and enhanced using the non-linear power law describing rate effects (Equation (1)), to give the

ultimate dynamic shaft resistance. The ultimate static resistance at the pile tip is evaluated using the conventional expression of 9 c_u, and enhanced by the corresponding rate effect coefficient to give the ultimate dynamic tip resistance.

The dynamic forces calculated for the soil springs are then compared with the ultimate dynamic forces. If the calculated force in each spring does not exceed the ultimate dynamic force, the soil behaviour remains linear elastic. This implies that there is still sufficient bond between the soil and the pile that elastic waves can propagate across the soil-pile interface and greater shear stresses can be induced into the soil, changing the pore pressures. If the calculated force equals or exceeds the ultimate force, the soil has reached the plastic range. The soil-pile interface has reached failure, and the propagation of elastic waves across the soil-pile interface ceases. Further shear stresses cannot be mobilised in the soil, and pore pressures no longer vary.

In the numerical model, the change from linear-elastic to plastic behaviour is implemented simply by disconnecting the appropriate dashpots. The dashpots are reconnected if the calculated dynamic spring force drops below the ultimate dynamic force, and the propagation of elastic shear waves resumes across the soil-pile interface.

6. COMPARISON WITH FIELD TESTS

Rigden et al. (1979) and Dolwin et al. (1979) reported comprehensive full-scale field tests performed on two fully instrumented hollow steel piles embedded in an overconsolidated clay. The tests were carried out at a site at Cowden on the coast of Holderness, North of Kingston-upon-Hull, which has been used extensively by the Building Research Establishment as a test bed for the evaluation of the properties of glacial till, generally described as a stiff stony clay, and the performance of site investigation equipment. At the site there is a sequence of clay tills which were laid down during a series of glacial advances.

The undrained shear strength of the site soil was reported to be in the range from 110 to 150 kPa over the upper 10 m. Oedometer tests revealed that the overconsolidation ratio of the clay varies from about 50 at 2.5 m depth to about 4 at 9 m depth (Lehane and Jardine, 1994). As the watertable was about 1 m below the ground level; the soil is fully saturated and the pile driving model is applicable. The shear modulus of the clay was found to be in the range from 10 to 20 kPa, based on the results of a 865 mm diameter plate bearing test (Marsland and Powell, 1985). The parameters adopted in the analysis are presented in Appendix I.

Figure 3 shows the details of the instrumented piles, which are designated A and B. The two piles were identical except that pile A was open-ended, while pile B had a 25 mm thick base plate. The 457 mm diameter piles were driven to a depth of 9.144 m by means of a BSP H.A. hammer with a ram mass of 3.5 t. The final height of the internal soil plug in the open-ended pile A was about 40 % of the penetration depth.

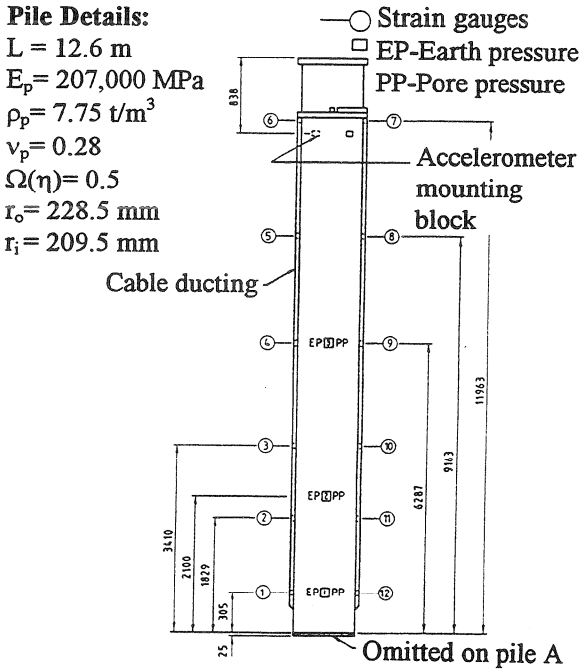

Figure 3. Test piles and instrumentation (after Rigden et al., 1979).

The pile instrumentation included strain gauge pairs, and earth and pore pressure cells mounted in the pile wall, flush with the outer face of the pile. Rigden et al. (1979) reported that while the strain gauges generally performed well, the data obtained during pile driving from the earth pressure cells were of limited use due to their slow response. Furthermore, several of the cells appeared to have suffered from significant zero drift during driving, even before they entered the ground. The data obtained from the pore pressure cells suggested that the majority of them retained some air. Although the pressure cell data are not fully reliable, they are adequate to provide general trends. For example, the immediate response of the cells to pile driving was a reduction in both the total earth pressure and pore pressure. The immediate reduction in these pressures may be attributed to the dilation which occurs on loading overconsolidated clays.

Figure 4 shows the irrecoverable pile tip displacement (set) for pile A, both measured and calculated using the pile driving model. The measured and final calculated sets for pile A are 7.6 mm/blow and 7.3 mm/blow, respectively. The longitudinal driving stresses at full penetration calculated using the pile driving model are compared with the measured values on Figure 5. There is a large discrepancy between the measured and calculated stresses at 6.287 m from the tip of pile A. Dolwin et al. (1979) suggested that this might be attributable to a poor weld between the

pressure cell flange and the pile at this location. However, there is a generally good agreement between the measured and calculated results.

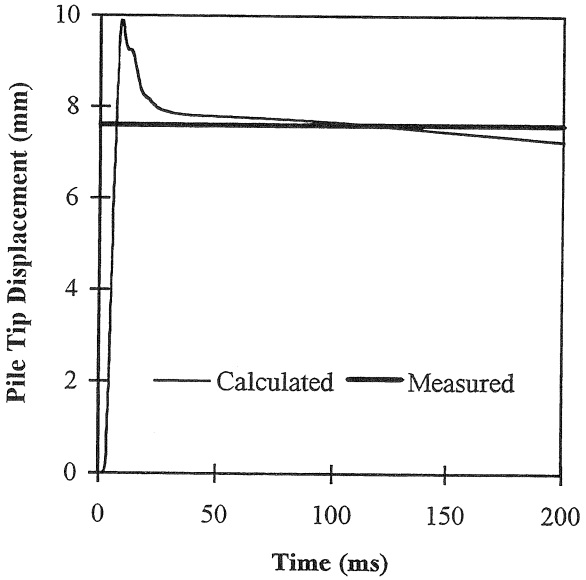

Figure 4. Comparison of measured and calculated sets for pile A.

7. CONCLUSION

A one-dimensional, finite element pile driving model has been presented. It incorporates soil failure governed by effective stresses and the Mohr-Coulomb strength criterion, rather than the more usual empirically-based criteria. Elasto-dynamic theory has been used to account for the loss of energy in the soil due to radiation damping. Rate effects have been incorporated using an empirically-based non-linear power law, which deals with the rapid loading imposed by pile driving.

The fundamental soil mechanics parameters involved in the model are the soil shear modulus, the soil density, Poisson's ratio of the soil, and the rate effect coefficients. The soil-pile interface parameters incorporated in the model are the drained adhesion and the friction angle between the pile material and the soil, which account for the limited bond at the interface. The change in radial total stress and pore pressure resulting from the expansion and contraction of the pile cross-section are computed and used to determine the normal effective stress acting on the pile.

The model was used to calculate the set and driving stresses induced in an instrumented pile embedded in an saturated, overconsolidated clay till. Encouraging agreement was obtained between the measured and calculated results, verifying the pile driving model.

8. APPENDIX I - SOIL DATA FOR CASE STUDY

8.1 Rate Effect Parameters

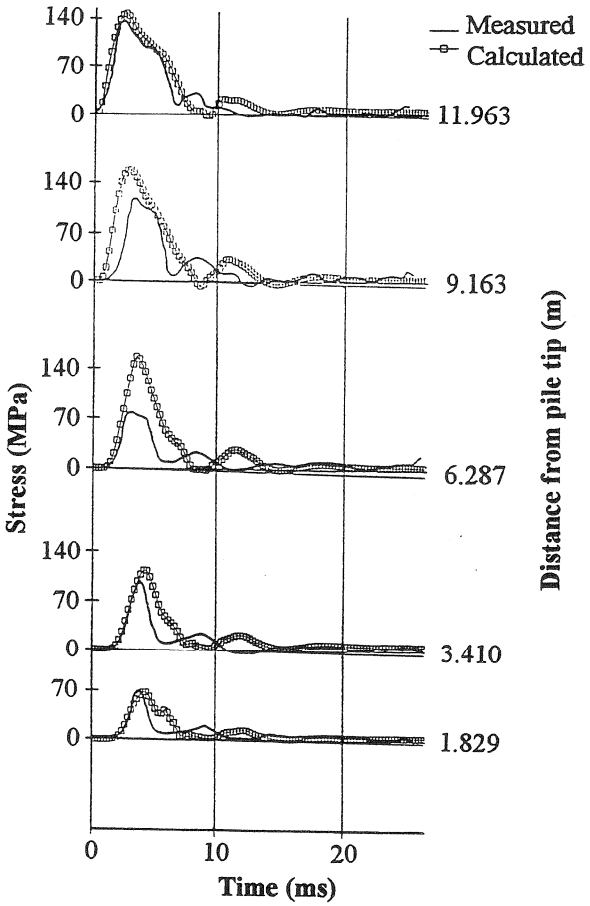

Figure 5. Comparison of measured and calculated driving stresses for pile A at full penetration.

J_s	=	1.03 s/m
N_s	=	0.268
J_p	=	0.386 s/m
N_p	=	0.404

where s denotes the pile shaft and p denotes the pile tip.

8.2 Soil Properties

ν_s	=	0.5
ρ_s	=	1.8 t/m^3
G_s	=	16,000 kN/m^2
c_u	=	115 kPa
A	=	0.27
m_1	=	1.07
m_2	=	1

8.3 Interface Parameters

c_a'	=	5 kPa
δ	=	20 deg

8.4 Hammer Details

Mass of Ram	=	3.5 t
Mass of Anvil	=	0.53 t
Impact Velocity	=	4.14 m/s

Cushion Stiffness	=	1,000,000 kN/m
Restitution Coefficient	=	0.9

9. REFERENCES

Bathe, K.J., and Wilson, E.L. (1976). *Numerical Methods in Finite Element Analysis*, Prentice-Hall, Englewood Cliffs.

Bjerrum, L. (1969). Pore pressure developed during undrained loading, in soil mechanics. *In: Soil Mechanics*, eds. T.W. Lambe and R.V. Whitman, Ch. 26, Wiley, New York.

Coyle, H.M., and Gibson, G.C. (1970). Empirical damping constant for sands and clays. *Proceedings ASCE, Journal of Soil Mechanics and Foundation Division*, Vol. 96, No. SM3, pp. 949-965.

Dolwin, J., Leonard, C.L., and Poskitt, T.J. (1979). A study of two instrumented piles during driving. Paper No. E2006, *Department of Civil Engineering, Queen Mary College, University of London, U.K.*

Egorov, K.E. (1965). Calculation of bed for foundation with ring footing. *Proceedings of Sixth International Conference on Soil Mechanics and Foundation Engineering, Toronto*, Vol. 2, pp. 41-45.

Gazetas, G., and Dobry, R. (1984). Simple radiation damping model for piles and footings. *Proceedings of ASCE, Journal of Engineering Mechanics*, Vol. 110, No. 6, pp. 937-956.

Henkel, D.J. (1960). The shear strength of saturated remoulded clays. *Proceedings of Conference on Shear Strength of Cohesive Soils, Boulder, Colorado*, p. 551.

Lee, S.L., Chow, Y.K., Karunaratne, G.P., and Wong, K.Y. (1988). Rational wave equation model for pile-driving analysis. *Proceedings of ASCE, Journal of Geotechnical Engineering Division*, Vol. 114, No. 3, pp. 306-325.

Lehane, B.M., and Jardine, R.J. (1994). Displacement pile behaviour in glacial clay. *Canadian Geotechnical Journal*, Vol. 31, pp. 79-90.

Litkouhi, S., and Poskitt, T.J. (1980). Damping constants for pile driveability calculations. *Geotechnique*, Vol. 30, No. 1, pp. 77-86.

Lysmer, J., and Richart, F.E. (1966). Dynamic response of footing to vertical loading. *Proceedings of ASCE, Journal of Soil Mechanics and Foundation Division*, Vol. 2, No. 1, pp. 65-91.

Marsland, A., and Powell, J.J.M. (1985). Field and laboratory investigations of the clay tills at the Building Research Establishment Test Site at Cowden Holderness. *Proceedings of International Conference on Construction in Glacial Tills and Boulder Clays, London,* pp. 147-168.

Novak, M. (1974). Dynamic stiffness and damping of piles. *Canadian Geotechnical Journal*, Vol. 11, pp. 574-598.

Novak, M., Nogami, T., and Aboul-Ella, F. (1978). Dynamic soil reactions for plane strain case. *Proceedings of ASCE, Journal of Engineering Mechanics*, Vol. 104, No. 4, pp. 953-959.

Rigden, W.J., Pettit, J.J., St. John, H.D., and Poskitt, T.J. (1979). Developments in piling for offshore structures. *Proceedings of Second International Conference on the Behaviour of Offshore Structures, London*, Vol. 2, pp. 279-296.

Smith, E.A.L. (1960). Pile driving analysis by the wave equation. *Proceedings of ASCE, Journal of Soil Mechanics and Foundation Division*, Vol. 86, No. 4, pp. 35-61.

Smith, I.M. (1988). *Programming the Finite Element Method*, Wiley, New York.